

# Theoretical analysis of peptidyl $\alpha$ -ketoheterocyclic inhibitors of human neutrophil elastase: Insight into the mechanism of inhibition and the application of QM/MM calculations in structure-based drug design

M. Paul Gleeson, Ian H. Hillier and Neil A. Burton\*

Department of Chemistry, University of Manchester, Oxford Road, Manchester, United Kingdom M13 9PL. E-mail: neil.burton@man.ac.uk; Fax: +44 161 275 4734; Tel: +44 161 275 4686

Received 17th February 2004, Accepted 18th June 2004  
First published as an Advance Article on the web 19th July 2004

It has been suggested from QSAR data (P. D. Edwards, D. J. Wolanin, D.A. Andisik and M. W. Davis, *J. Med. Chem.*, 1995, **38**, 76) that the inhibition of elastase by peptidyl  $\alpha$ -ketoheterocyclic inhibitors can occur in two ways, the less potent inhibitors forming a non-bonded Michaelis complex and the more potent set a covalently bonded enzyme–substrate intermediate. We report QM/MM studies of both binding and reactivity that confirm these findings, showing that the activity of the least potent set of inhibitors correlates with the calculated binding energy, and that of the more potent set correlates with the stability of the intermediate. These calculations show that QM/MM methods can be successfully employed to understand complicated structure–activity relationships and might be employed in the design and assessment of new inhibitors.

## Introduction

Computer simulation studies of substrate–protein interactions are now recognized as a valuable aid to drug discovery. The potency of potential inhibitors is traditionally determined using either estimates of the free energy of substrate–protein binding using intermolecular potentials<sup>1–5</sup> or, to achieve greater computational throughput, more phenomenological scoring functions may be employed.<sup>6–9</sup> Although the latter may not describe the individual interactions which contribute to the binding energy particularly accurately, they have been successful in predicting relative overall binding affinities to complement experimental high throughput screening strategies. More rigorous modeling methods, particularly those employing quantum mechanics, do not feature strongly in the current drug discovery process, perhaps due to the perception that such computationally demanding methods do not yield results relevant to drug discovery commensurate with their computational cost. However, in addition to providing, in principle, more accurate non-covalent potentials due in part to the explicit inclusion of electronic polarisation, quantum mechanical methods are needed to describe reactive processes where covalent interactions develop between a substrate and the protein.

In order to model such covalent interactions at the essential level of accuracy, without requiring unrealistic computational resources, hybrid methods are now widely employed. Here, those parts of the system where electron reorganization is crucial, usually the enzyme active site and those parts of the substrate directly involved in interactions with the protein, are treated at an appropriate level of quantum mechanics (QM). The remainder of the system, where electronic effects are much less important, is modelled at a less computationally demanding level, such as using a molecular mechanical (MM) force field. This allows for the inclusion of the steric and electrostatic role of the enzyme on the reaction occurring at the active site. Thus, unlike quantum mechanical calculations of the often small reactive region or those employing uniform dielectric fields to describe the environment, these hybrid QM/MM methods include explicit interactions with the protein and are now being widely used to understand novel enzyme mechanisms such as the quantum behaviour of hydrogen tunnelling in a number of enzymes.<sup>10,11</sup> They have also been shown to be particularly effective in understanding the mechanisms of inhibition which require the description of a transition state analogue.<sup>12</sup>

Here we shall explore the value of these QM/MM methods<sup>13–15</sup> as an aid to drug discovery<sup>12,16</sup> by using them to help understand

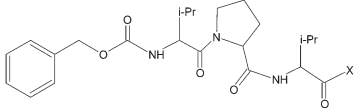
the molecular origins of the different biological activities of a series of inhibitors of a serine protease. Peptidyl  $\alpha$ -ketoheterocycles are known to inhibit the serine protease, human neutrophil elastase (HNE)<sup>17</sup> which is a major component of the inflammatory defense system. Edwards *et al.*<sup>18,19</sup> have found the activities of these compounds to vary quite widely with subtle changes in molecular structure, and reported inhibition constants ( $K_i$ ) ranging from 28 nM to 88 000 nM (see Table 1). There are two general ways in which electrophilic ketones can inhibit HNE (see Fig. 1); the first is by the formation of a stable Michaelis complex involving only non-covalent interactions between the inhibitor and the enzyme. The second possibility involves bond breaking and formation associated with nucleophilic attack of the inhibitor by the serine residue of the protease catalytic triad,<sup>20,21</sup> following its deprotonation by histidine, leading to a covalent tetrahedral intermediate.<sup>22,23</sup> This mechanism has been well studied by others<sup>24–27</sup> for the natural substrate and may occur in either a stepwise or concerted fashion.<sup>28–30</sup> The next step in the conventional catalytic serine protease mechanism, that of the decomposition of the tetrahedral intermediate and hydrolysis of the peptide bond, cannot occur for the ketonic inhibitors as their (C–C) bond is much stronger than the equivalent (C–N) bond of a natural substrate.<sup>31</sup> Edwards *et al.*<sup>18</sup> have suggested a link between inhibitor-potency and the electron withdrawing ability of the heterocyclic ring based on a limited quantitative–structure activity relationship (QSAR) relating Charton  $\sigma_1$ -values<sup>32</sup> to the inhibition constants. It was argued that a correlation between potency and the electron withdrawing ability of the rings would only be observed for inhibitors that form a tetrahedral intermediate. In these cases the electron withdrawing group is just two bonds away from the oxyanion and provides stabilization of the intermediate *via* the inductive removal of electron density. Inhibitors that function by formation of a non-bonded Michaelis complex only cannot be distinguished in this way. The experimental data, although not conclusive, with a number of unexplained outliers, do show that inhibitors with the largest sigma values are found to be the most potent. These conclusions will now be explored in greater detail using a combination of standard MM and hybrid QM/MM computational methods.

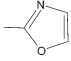
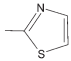
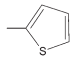
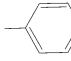
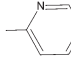
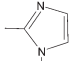
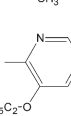
## Computational procedures

### Model preparation

Computational studies have been carried out to model both non-covalent and reactive inhibition mechanisms of the seven HNE

**Table 1** Peptidyl  $\alpha$ -keto-heterocyclic inhibitors, their experimental  $K_i$  (in nM) and  $\sigma_I$ -values



Inhibitor No.	Heterocycle (X)	$K_i$ /nM	$\sigma_I$ -value
1		28	0.38
2		270	0.34
3		4300	0.19
4		16000	0.12
5		22000	0.18
6		80000	0.27
7		88000	—

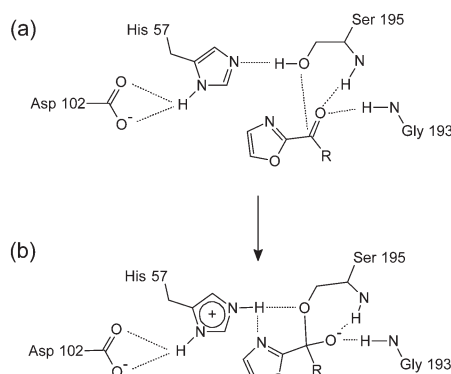


**Fig. 1** Two potential modes of HNE inhibition by the peptidyl  $\alpha$ -keto-heterocyclic compounds: via a Michaelis complex or via a stable tetrahedral intermediate.

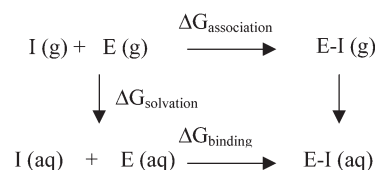
inhibitors shown in Table 1, which were chosen such that the wide potency range was sampled as evenly as possible. The first mode of inhibition, that of formation of the Michaelis complex, has been studied using molecular mechanics with the conventional AMBER force field,<sup>33</sup> and with the QM/MM method for comparison. The second mode of inhibition was studied using the combined QM/MM method since it involves the formation of a tetrahedral intermediate. To study the equilibrium between the Michaelis complex and the tetrahedral complex, we shall consider the energy difference between the respective minimum energy structures rather than employing a full conformational treatment to obtain free energies. As such, our approach is considerably less computationally demanding and is more appropriate for rapid screening of candidate drug molecules. Neglect of entropic effects is unlikely to affect our findings since all of the inhibitors are expected to bind in a similar conformation with little structural change.

Since no crystal structure of a peptidyl  $\alpha$ -keto-heterocyclic inhibitor bound to HNE was available, initial models of the inhibitors in the active site were constructed from an X-ray crystal structure of HNE complexed to a chloromethyl ketone-inhibitor (CCl<sub>3</sub>-Val-

Pro-Ala-Ala-methoxy succinyl, 1PPG resolved to 2.3 Å).<sup>34</sup> This substrate binds in a similar orientation within the active site as turkey ovomucoid inhibitor,<sup>17</sup> used in our earlier inhibitor binding study.<sup>16</sup> Significant conformational change is not likely since the chloromethyl ketone-inhibitor is structurally very similar to the peptidyl  $\alpha$ -keto-heterocyclic inhibitors (X-Val-Pro-Val-Cbz) studied here, the primary difference being the replacement of the chloromethyl group with a range of heterocyclic rings, denoted (X) in Table 1. The inhibitors to be studied were approximated by smaller models, (X-Val-Pro-CH<sub>3</sub>), which are large enough to ensure a correct binding orientation within the active site. These models retain the major interactions of the substrate with the catalytic triad and oxy-anion hole, namely the valine i-Pr sidechain with the S<sub>1</sub> pocket, and the secondary interaction of the valine peptide NH with the S<sub>2</sub> position.<sup>17</sup> A model of an amide natural substrate (CH<sub>3</sub>-Ala-Val-Nmethylacetamide) was also considered for purposes of comparison.

Initial enzyme-substrate models were generated using molecular dynamics (MD) simulations and subsequent minimisation, using the AMBER force field to remove spurious binding interactions. The non-standard parameters required for the unsaturated rings were based on similar species in the standard database, whilst torsional parameters for the barrier to rotation about the heterocycle-carbonyl groups were modified to give values in line with those of the gas phase substrate at the HF/6-31G(d) level. ESP atomic charges<sup>35</sup> were obtained for each substrate at the HF/6-31G(d) level. The enzyme-substrate models were solvated in a box of approximately 4500 TIP3P<sup>36</sup> water molecules, equilibrated to 300 K using 10 ps of MD and a 1 fs timestep, a 12 Å VDW cut-off, constant pressure and periodic boundary conditions. This was followed by full minimization at the MM level to a rms deviation in the gradients of less than  $1 \times 10^{-2}$  kcal mol<sup>-1</sup> Å<sup>-1</sup>. Inhibitor-solvent models were also created using a box of approximately 400 TIP3P water molecules and equilibrated using the same protocols described above.

To estimate the net binding energy of each inhibitor, I (aq), to form the Michaelis complex in solution, E-I (aq), we should consider the effects of desolvation of the inhibitor and the full thermodynamic cycle:



However, here we shall only consider the relative binding affinities of related inhibitors, and so the contributions can be simplified. The relative difference of solvation,  $\Delta\Delta G_{\text{solvation}}$ , of two similar inhibitors, I1 relative to I2, will be approximated by

$$\Delta\Delta G_{\text{solvation}} \approx E_{\text{int}}(\text{I2, aq}) - E_{\text{int}}(\text{I1, aq})$$

The relative association energies,  $\Delta\Delta G_{\text{association}}$ , can be similarly approximated by

$$\Delta\Delta G_{\text{association}} \approx E_{\text{int}}(\text{I2, enzyme}) - E_{\text{int}}(\text{I1, enzyme}),$$

provided that the two inhibitors bind with similar distortion effects.  $E_{\text{int}}(\text{I, aq})$  and  $E_{\text{int}}(\text{I, enzyme})$  are the potential energies of interaction of an inhibitor, I, with water and enzyme environments respectively. These are taken from the optimized enzyme-inhibitor and solution-inhibitor structures at the MM level by re-evaluation of the van der Waals and electrostatic interaction energies of the inhibitor with the enzyme and solvent in each case. Since the number of atoms in the enzyme or solvent are the same for each inhibitor, taking the difference in these interaction energies gives us an estimate of the relative binding energy,

$$\Delta\Delta G_{\text{binding}} = \Delta\Delta G_{\text{association}} - \Delta\Delta G_{\text{solvation}}$$

which will be positive if I1 is a better inhibitor than I2.

## QM/MM calculations

We have employed the PM3 Hamiltonian for the bulk of the QM/MM calculations since it has previously been shown to be as effective as *ab initio* methods for describing intrinsic substituent effects on the acidity of a variety of systems.<sup>37</sup> As a similar substituent effect is expected to operate in this case to control the electrophilicity of these inhibitors, the PM3 method should give relative energetics of sufficient accuracy to differentiate between the two mechanisms. The QM/MM program, which couples the AMBER<sup>38</sup> and Gaussian94<sup>39</sup> programs together, has been described previously,<sup>13</sup> together with the way of 'linking' the QM and MM regions across a covalent junction. Initial QM/MM models of the Michaelis complexes of the seven inhibitors and of the natural substrate were constructed from the minimised MM structures. All atoms (except link atoms) within the QM regions were fully geometry optimized in the presence of the enzyme environment.

Relative binding energies of the substrates at the QM/MM level were computed in a similar way to the classical MM estimates, using the same enzyme and solution configurations. In each case the geometry of each substrate was fully optimized within both the enzyme and solution at the QM/MM level using the PM3 (QM) Hamiltonian and the environment used in the MM study. In these calculations the net binding energy will include changes in the internal energy of the inhibitor arising from both geometric distortion and electronic polarization due to interaction with the environment, which are absent in the classical MM studies.

We now describe the QM/MM calculations carried out to investigate the alternative inhibition mechanism, that of formation of the tetrahedral intermediate. Here it is necessary to use a quite extensive QM region (Fig. 2) such that the most important residues in the active site are treated quantum mechanically. The QM region comprised the substrate (X–Val–Pro–CH<sub>3</sub>), the functional groups of the catalytic triad (Asp102, His 57) and the oxy-anion hole (Gly 193, Ser 195 and backbone of Asp 194). This gives a QM region of between 90–95 atoms depending on the inhibitor. Hydrogen (link) atoms<sup>40</sup> were used to terminate either the C<sub>α</sub> or C<sub>β</sub> (Fig. 2) atoms in the residues that occur at the boundary between the QM and MM regions. Optimised structures for the tetrahedral complexes for six inhibitors and the natural substrate were then found at the same level. This was not done for inhibitor 7 since the binding conformation of the bulky heterocycle prevents the formation of a hydrogen bond between His 57 and Ser 195 which is essential for the reaction to occur. The potential energy difference between the tetrahedral intermediate and the Michaelis complex, (the reaction energy), will be used to assess the potency of the inhibitors *via* a reactive mechanism. Large endothermic reaction energies will naturally favour binding of the Michaelis complex and the inhibition constants will depend less upon a reactive mechanism. A stable tetrahedral complex can potentially offer an alternative mechanism to lower inhibition constants and increase potency.

To study any differences in the reaction mechanism of the natural substrate and the most potent inhibitor 1, stationary points corresponding to the Michaelis complex, transition state and tetrahedral intermediate were calculated along each reaction pathway. Potential energy surfaces (PES) were also constructed by varying the two

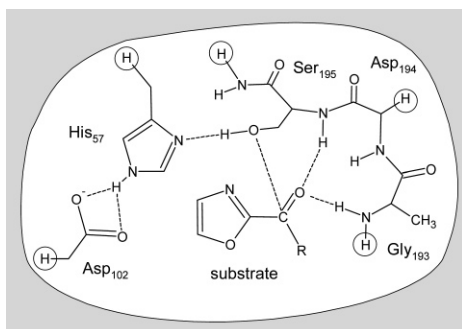


**Fig. 2** QM region used in the QM/MM calculations. Inhibitor 1 is shown where R is Val–Pro–CH<sub>3</sub>. Link atoms are circled.

**Table 2** QM/MM and MM enzyme binding energies (in kcal mol<sup>-1</sup>) relative to the inhibitor 7

Inhibitor	QM/MM binding energy	MM binding energy
1	3.8	8.3
2	4.6	5.1
3	10.5	15.2
4	6.8	7.4
5	1.9	1.8
6	6.3	5.3
7	0.0	0.0

distances associated with the bond breaking and forming parts of the reaction, namely the distance between the N<sub>(δ2)</sub> atom of His 57 and the hydroxyl hydrogen of Ser 195, and that between the hydroxyl oxygen of Ser 195 and the carbonyl carbon of the substrate. Both these distances were incremented in steps of approximately 0.3 Å from the Michaelis complex to the tetrahedral intermediate structure and at each point the remaining geometrical parameters were optimised. The transition states and intermediates on the surface were subsequently refined without restraints and characterized as minima or transition states by the calculation of vibrational frequencies.

To assess the reliability of the PM3 Hamiltonian used in these calculations, the reaction between the natural substrate and the enzyme was studied using a density functional method involving the B3LYP functional and a 6–31G(d) basis set.

## Results and discussion

### Inhibitor binding energies

We first discuss the enzyme–inhibitor binding energies which will be a reflection of the relative preference of the inhibitor for either the aqueous phase or for the enzyme. As previously noted, our approach will neglect entropic effects which we would only expect to be important for substrates which are structurally diverse.<sup>1,41–43</sup> In our studies non-enthalpic effects should be similar due to the considerable homology of the inhibitors which are all neutral, of similar size and quite hydrophobic, differing only in their heterocyclic rings.

In Table 2 we present binding energies for the series of inhibitors relative to the least potent inhibitor, 7. The correlation between  $\ln K_i$  and binding energies is similar for both MM and QM/MM models. We see that for the weaker inhibitors (3 to 7) with  $K_i$  values above 4000 nM there is a good correlation between the binding energy and  $\ln K_i$ , which is absent for the more potent inhibitors (1 and 2) (Fig. 3). The binding energy of inhibitor 6 is found to correlate poorly with the experimental  $K_i$  value, possibly as a result of more subtle free energy and desolvation effects which are not included here. This inhibitor has a significant effect on the statistical error of our correlations due to the relatively small number of data points used. The QM/MM results do not show any improvement over the MM method and the R<sup>2</sup> values associated with the QM/MM and MM correlations are 0.54 and 0.69, respectively.

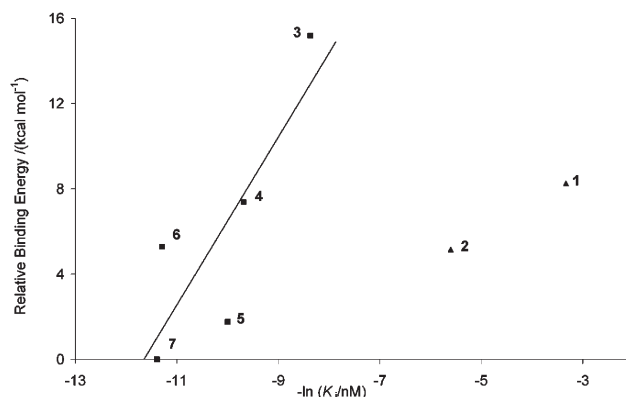


**Fig. 3** Plot of  $-\ln(K_i)$  against binding energy (relative to inhibitor 7) at the MM level. Inhibitors 1–2 are represented by triangles and inhibitors 3–7 by squares.

**Table 3** Relative energies (in kcal mol<sup>-1</sup>) of stationary states on the natural substrate reaction potential energy surface relative to the Michaelis complex at the QM(PM3)/MM and QM(B3LYP/6-31G(d))/PM3/MM levels.

Structure <sup>a</sup>	PM3 energy	B3LYP/6-31G(d) energy
MICO	0.0	0.0
TS1	21.6	7.7
PT-MICO	15.6	12.4
TS2	27.2	30.1
TET	24.6	26.0

<sup>a</sup>Michaelis complex (MICO), transition state 1 (TS1), proton transfer Michaelis complex (PTMICO), transition state 2 (TS2) and the tetrahedral intermediate (TET).

The data in Table 2 show that the six inhibitors interact with the enzyme almost to the same extent although closer inspection of the absolute interaction energies shows that there is less variation between the MM interaction energies for the enzyme (74.5 ± 1.9 kcal mol<sup>-1</sup>) than for solution (71.7 ± 4.5 kcal mol<sup>-1</sup>). This is because the total interaction energy is dominated by the common peptide fragment. In the Michaelis complex there is little flexibility to allow the more polar heterocyclic rings to assume more favourable conformations. However in solution the heterocyclic rings have more freedom to interact with the mobile water molecules and thus largely dictate the overall binding energies. We can see that inhibitors 1, 2 and 6 have moderate binding energies and that each interacts with solution and the enzyme to a similar extent. Inhibitors 3 and 4, and to a lesser extent 5, interact better with the enzyme relative to solution, resulting in greater binding energies. Conversely, the sterically hindered inhibitor 7 interacts much better with solution than the enzyme, reducing its affinity for the enzyme significantly.

Interestingly, inhibitor 4 is found to be more potent than 5, in agreement with experiment, even though it does not have as many hydrogen bond donors to interact within the active site. It is unlikely that the increased potency of 4 relative to 5 can be attributed to its greater reactivity since it also has a less electron withdrawing heterocycle and we would expect it to form a less exothermic tetrahedral intermediate. The reason for the increased potency of 4 is likely to be a result of its greater affinity for the enzyme than solution due to its relative hydrophobicity and not due to a more complimentary active site structure. This can be seen when the interaction energies are decomposed showing that although the pyridine ring of 5 interacts better with the enzyme than does the phenyl ring of 4 (by ~2 kcal mol<sup>-1</sup>), inhibitor 5 also interacts with solution (by ~7.7 kcal mol<sup>-1</sup>) more strongly than 4. Thus the net effect is that binding of 4 is more favourable by ~5.6 kcal mol<sup>-1</sup>.

Overall the calculated interaction energies suggest that the less potent set of inhibitors (3 to 7) inhibit *via* a binding mode and the more potent set (1 and 2) do not. While the binding energies do not provide insight into the mechanism of inhibition of the more potent set, they do show that if we wish to explain the activity of the more potent set *via* a binding mechanism, their binding energies would need to be considerably larger than those of the most strongly bound inhibitors, in the region of 24 to 40 kcal mol<sup>-1</sup> relative to inhibitor 7. Furthermore, we find the cut-off between those that inhibit *via* binding and those that do not to be between 300–4000 nM which is in good agreement with the 1000 nM cutoff suggested by Edwards *et al.*<sup>19</sup> Unfortunately, it was not possible to narrow this range further due to the lack of any measured inhibitors in this range. We next consider the inhibitors in terms of their relative reactivities.

### Inhibitor reactivity

We first discuss the accuracy of the PM3 Hamiltonian<sup>44</sup> by comparing the reaction energies for the formation of a tetrahedral intermediate from the natural substrate at this level and at the higher B3LYP/6-31G(d) level.<sup>45,46</sup> In table 3 we present energies for the stationary points relative to the Michaelis complex (MICO) found with the QM(PM3)/MM method. Energies at the QM(B3LYP/6-31G(d))/MM level at these geometries are shown for comparison. The first

**Table 4** Reaction energies and the barrier heights (kcal mol<sup>-1</sup>) for the six inhibitors using the QM(PM3)/MM method

Inhibitor no.	Reaction energy	Forward Barrier
1	5.2	21.0
2	6.4	22.5
3	11.4	23.6
4	19.5	23.7
5	16.6	24.9
6	12.2	22.3

step, corresponding to transfer of a proton from Ser 195 to His 57 to form a structure labelled PTMICO (*via* transition state TS1), requires 15.6 kcal mol<sup>-1</sup> at the PM3 level which is slightly greater than the value found by others.<sup>28</sup> At the B3LYP/6-31G(d)/PM3 level a comparable value of 12.4 kcal mol<sup>-1</sup> was found but the lower energy of the TS1 structure suggests that the higher energy PM3 stationary point corresponding to PTMICO is likely to be an artifact of the semi-empirical method. Full optimization at the HF/3-21G level shows that PTMICO is not a minimum at a higher level. This discrepancy will not affect our discussions regarding the relative reactivity of the inhibitors since this step is not rate determining.

If we compare the overall reaction barrier corresponding to subsequent nucleophilic attack *via* transition state (TS2), and the overall reaction energy to form the tetrahedral intermediate (TET), we note that the PM3 energies are not significantly different to those at the B3LYP/6-31G(d) level, the reaction barriers being 27.2 and 30.1 kcal mol<sup>-1</sup> at the two levels respectively. The reaction energies are in even closer agreement, 24.6 and 26.0 kcal mol<sup>-1</sup> respectively, giving us confidence that the PM3 method can predict the relative reactivity of the inhibitors.

### Inhibitor-tetrahedral complex

We now turn our attention to the study of an inhibition mechanism through reaction to form an unreactive tetrahedral complex, analogous to the tetrahedral intermediate which is formed with the natural substrate. Although the potency of reactive inhibitors will depend to some extent upon the forward and backward barrier heights, for similarly reactive inhibitors we might expect the potency to be particularly influenced by the competitive binding of the tetrahedral and Michaelis complexes as a result of their relative thermodynamic stabilities. Table 4 summarises the calculated reaction energies (energies of the tetrahedral complexes relative to those of the Michaelis complexes) and the forward barrier heights. The barrier heights are similar for all of the inhibitors considered, indicating that their value does not control the degree of inhibition.

On analysis of the reaction energies to form the six tetrahedral complexes (1–6) (Fig. 4) we find that inhibitors 1 and 2 form less endothermic intermediates than 3 to 6 which correlates with their large experimental potency. There does not appear to be a strong correlation between the reaction energies and experimental potencies of the set 4 to 6 which adds further support to the suggestion that the activity of this set is primarily determined by formation of a non-bonded Michaelis complex in agreement with the findings of our binding study. However, we do not rule out the possibility that the activity of these ketonic inhibitors may arise from both mechanisms seeing that inhibitor 3 has the lowest predicted binding energy and is also found to be moderately reactive. Since the only structural differences between the six inhibitors are the heterocyclic rings we show a plot of the  $\sigma_1$ -value of the rings against the reaction energy (Fig. 5). We observe a strong correlation although there is no correlation of potency ( $K_i$ ) with the reaction energy for those above the cut-off value of 1000 nM. We also show in Fig. 6 that the experimentally derived  $\sigma_1$ -values of the heterocyclic rings do indeed follow the computed absolute charge of the heterocycles in the tetrahedral intermediate so that the greater the inductive removal of electron density from the oxyanion onto the heterocyclic rings, the more stable is the intermediate.

Thus, our calculations suggest that for potent inhibition of HNE, ketonic heterocyclic inhibitors need  $\sigma_1$  values greater than ~0.30

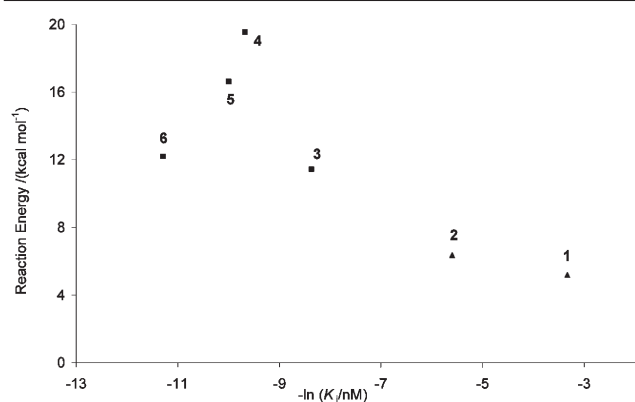


**Fig. 4** QM(PM3)/MM reaction energies (in kcal mol<sup>-1</sup>) plotted against  $-\ln(K/nM)$ .

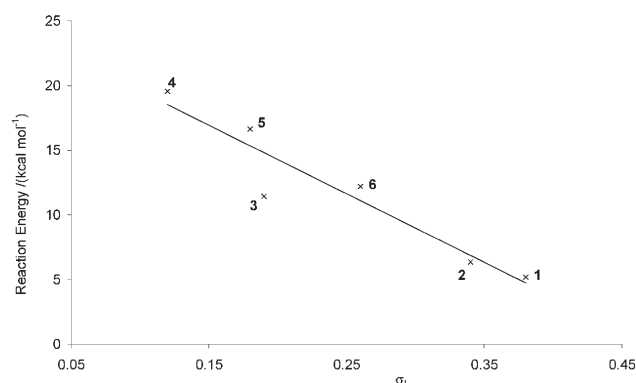


**Fig. 5** QM(PM3)/MM reaction energies plotted against the  $\sigma_1$  value of the heterocycle.

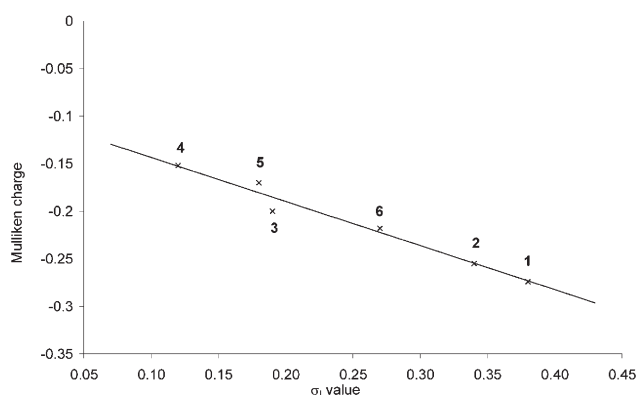


**Fig. 6** The total Mulliken charge of the heterocycle plotted against  $\sigma_1$ .

for formation of a stable tetrahedral intermediate. However this effectively means the potency of this type of inhibitor will be restricted to the  $\mu\text{M}$  range given that there is a limit on how electron withdrawing small heterocyclic rings can be.

Since the heterocyclic rings inductively remove electron density through the  $\sigma$ -bond network, we do not observe this stabilizing effect in the transition states (Table 4), where the (C–O) bond of the substrate is not fully formed. This means that the majority of the active site negative charge is maintained on the serine nucleophile and not on the substrate carbonyl, preventing the heterocyclic rings from inductively removing electron density to the same extent observed in the tetrahedral intermediate. This explains why all of the transition states are found at a similar energy (21–25 kcal mol<sup>-1</sup>) compared to the Michaelis complexes.

In general, the tetrahedral complexes optimized at the QM/MM level are similar to X-ray crystal structures reported by Edwards *et al.*<sup>18</sup> These include two strong hydrogen-bonds between the oxyanion and oxyanion hole and the formation of an interaction, where possible, between the inhibitor heterocycle and the protonated imidazolium cation of His 57. For example, our

computed tetrahedral intermediate of inhibitor 1, which has an oxazole heterocycle attached to its valine carbonyl, is remarkably similar to the experimental X-ray crystal structure of porcine pancreatic elastase complexed with a peptidyl  $\alpha$ -keto-benzoxazole inhibitor.<sup>18</sup> In this case the key interaction between His 57 N<sub>(62)</sub> and N<sub>(2)</sub> of the oxazole inhibitor is found to be at 3.0 Å in good quantitative agreement with the experimental distance of 2.8 Å for the benzoxazole inhibitor.

### Mechanistic pathways

In Fig. 7 we plot potential energy surfaces corresponding to (a) the natural substrate and (b) inhibitor 1 for the proton transfer and nucleophilic attack. The approximate minimum energy pathways, leading from the Michaelis complex to the tetrahedral complex for each substrate can be seen to vary considerably in character. Nucleophilic attack by Ser 195 on the carbonyl of the natural substrate is a higher energy process than proton transfer from Ser 195 to His 57. In contrast, for inhibitor 1 both processes are quite similar energetically. The energy of the transition state for the natural substrate and inhibitor, relative to their Michaelis complexes, are 27.2 and 21.0 kcal mol<sup>-1</sup> respectively.

The differences between the two potential energy surfaces are most pronounced in the final stage of the nucleophilic (C–O) coordinate, between 2.2–1.5 Å, where the electron withdrawing effect of the inhibitor's heterocycle can begin to stabilize the

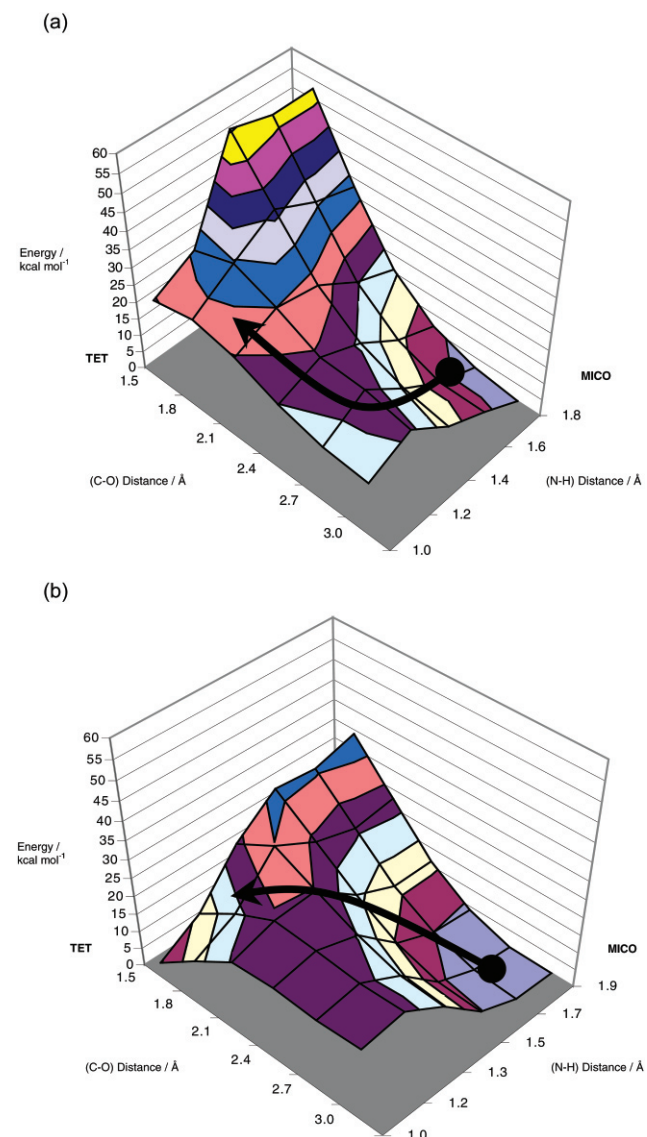


**Fig. 7** QM(PM3)/MM potential energy surfaces for the natural substrate and inhibitor 1. The black arrows represent approximate minimum energy pathways from the Michaelis complex (MICO) to the tetrahedral complex (TET).

resulting structures, particularly the increased oxyanion character of the carbonyl. Thus the transition state of the natural substrate, as noted previously,<sup>47</sup> is found close to the tetrahedral intermediate on the potential energy surface and is therefore energetically similar. The transition states of the inhibitors (1–6) are found to favour a more concerted mechanism with (C–O) distances between 2.11–2.22 Å, as opposed to 1.75 Å in the natural substrate.

Our minimum energy profile for the natural substrate conflicts with the original gas phase PM3 calculations of Daggett *et al.*,<sup>48</sup> but is in broad agreement with recent higher level QM/MM studies<sup>29,49</sup> which suggest a concerted reaction within the enzyme and which predict lower free energy barriers. We must therefore be cautious with regard to the absolute reaction profiles since, in the case of the natural substrate, the PM3 method does appear to predict a stable proton transfer intermediate although the surfaces are relatively flat in this region. Despite this uncertainty, comparison of the natural substrate and inhibitor potential energy surfaces does highlight potentially important differences in the profiles consistent with the stabilising effect of the heterocycle as the tetrahedral intermediate is formed.

## Conclusions

Prompted by the research of Edwards *et al.*,<sup>19</sup> binding energy and reactivity calculations have been performed on a series of inhibitors of HNE in an attempt to elucidate the mechanism of inhibition. Using QM/MM methods, we find that the potency of the inhibitors with the most electron withdrawing heterocycles correlates with the stability of the tetrahedral complexes whilst the potency of those inhibitors with only weakly electron withdrawing heterocycles and very endothermic reaction energies correlates with the calculated binding energy of the Michaelis complex. Thus we conclude that inhibitors with experimental  $K_i$  values above ~1000 nM will inhibit *via* a binding mode, while those with  $K_i$  values below 1000 nM will do so by reaction at the active site to form the tetrahedral complex (transition state analogue).

It is apparent from these results that the hybrid QM/MM technique may be successfully used to explain enzyme-inhibition mechanisms where a transition state analogue can form. Given that we can now routinely analyze relatively large numbers of molecules using the approach outlined in this paper, we believe the QM/MM method could now be reliably considered for predictive structure based drug design.

We thank EPSRC for support of this research.

## References

- 1 J. Åqvist, C. Medina and J. E. Samuelsson, *Protein Eng.*, 1994, **7**, 385.
- 2 A. C. Pierce and W. L. Jorgensen, *J. Med. Chem.*, 2001, **44**, 1043.
- 3 J. Wang, R. Dixon and P. A. Kollman, *Proteins*, 1999, **34**, 69.
- 4 J. P. Price and W. L. Jorgensen, *J. Comput.-Aid. Mol. Des.*, 2001, **15**, 681.
- 5 S. Huo, J. Wang, P. Cieplak, P. A. Kollman and I. D. Kuntz, *J. Med. Chem.*, 2002, **45**, 1412.
- 6 P. J. Goodford, *J. Med. Chem.*, 1985, **28**, 849.
- 7 S. Liang and N. V. Grishin, *Protein Sci.*, 2002, **11**, 322.
- 8 R. D. Head, M. L. Smythe, T. I. Oprea, C. L. Waller, S. M. Green and G. R. Marshall, *J. Am. Chem. Soc.*, 1996, **118**, 3959.
- 9 G. Jones, P. Willett, R. C. Glen, A. R. Leach and R. Taylor, *J. Mol. Biol.*, 1997, **267**, 727.
- 10 G. Tresadern, J. P. McNamara, M. Mohr, H. Wang, N. A. Burton and I. H. Hillier, *Chem. Phys. Lett.*, 2002, **358**, 489.
- 11 C. Alhambra, M. L. Sanchez, J. C. Corchado, J. Gao and D. G. Truhlar, *Chem. Phys. Lett.*, 2002, **355**, 388–394.
- 12 M. P. Gleeson, N. A. Burton and I. H. Hillier, *Chem. Commun.*, 2003, 2180.
- 13 M. J. Harrison, N. A. Burton and I. H. Hillier, *J. Am. Chem. Soc.*, 1997, **119**, 122.
- 14 A. Warshel and M. Levitt, *J. Mol. Biol.*, 1976, **103**, 227.
- 15 M. J. Field, P. A. Bash and M. Karplus, *J. Comput. Chem.*, 1990, **11**, 700.
- 16 G. Tresadern, P. F. Faulder, M. P. Gleeson, Z. Tai, G. MacKenzie, N. A. Burton and I. H. Hillier, *Theor. Chem. Acc.*, 2003, **109**, 108.
- 17 W. Bode, E. Meyer Jr. and J. C. Powers, *Biochemistry*, 1989, **28**, 1951.
- 18 P. D. Edwards, E. F. Meyer, J. Vijayalakshmi, P. A. Tuthill, D. A. Andisik, B. Gomes and A. Strimpler, *J. Am. Chem. Soc.*, 1992, **114**, 1854.
- 19 P. D. Edwards, D. J. Wolanin, D. A. Andisik and M. W. Davis, *J. Med. Chem.*, 1995, **38**, 76.
- 20 G. Dodson and A. Wlodawer, *Trends Biochem. Sci.*, 1998, **23**, 347.
- 21 J. Nishihira and H. Tachikawa, *J. Theo. Biol.*, 1999, **96**, 513.
- 22 M. Topf, P. Varnai, C. J. Schofield and W. G. Richards, *Proteins*, 2002, **47**, 357.
- 23 M. Shokhen and A. Albeck, *Proteins*, 2000, **40**, 154.
- 24 M. Topf, P. Varnai and W. G. Richards, *Theor. Chem. Acc.*, 2001, **106**, 146.
- 25 M. Topf, P. Varnai and W. G. Richards, *J. Am. Chem. Soc.*, 2002, **124**, 14780.
- 26 M. Topf, P. Varnai, C. J. Schofield and W. G. Richards, *Proteins*, 2002, **47**, 357.
- 27 Y. Zhang, J. Kua and J. A. McCammon, *J. Am. Chem. Soc.*, 2002, **124**, 10572.
- 28 S. Scheiner, W. N. Lipscomb and D. A. Kleier, *J. Am. Chem. Soc.*, 1976, **98**, 4770.
- 29 M. Strajbl, J. Florian and A. Warshel, *J. Am. Chem. Soc.*, 2000, **122**, 5354.
- 30 A. Warshel, S. Russell and F. Sussman, *Isr. J. Chem.*, 1986, **2**, 217.
- 31 A. R. Fersht, *Enzyme Structure and Mechanism*. W. H. Freeman & Co New York, 1985.
- 32 P. J. Taylor and A. R. Wait, *J. Chem. Soc., Perkin Trans. 2*, 1986, 1765.
- 33 W. D. Cornell, P. Cieplak, C. I. Bayly, I. R. Gould, K. M. Merz, D. M. Ferguson, D. C. Spellmeyer, T. Fox, J. W. Caldwell and P. A. Kollman, *J. Am. Chem. Soc.*, 1995, **117**, 5179.
- 34 W. An-Zhi, I. Mayr and W. Bode, *FEBS Lett.*, 1998, **234**, 367.
- 35 B. H. Besler, K. M. Merz and P. A. Kollman, *J. Comput. Chem.*, 1990, **11**, 431.
- 36 W. L. Jorgensen, J. Chandrasekhar, J. D. Madura, R. W. Impey and M. L. Klein, *J. Chem. Phys.*, 1983, **79**, 926.
- 37 R. Karaman, J. T. L. Huang and J. L. Fry, *J. Comput. Chem.*, 1990, **11**, 1009.
- 38 D. A. Pearlman, D. A. Case, J. W. Caldwell, W. S. Ross, T. E. Cheatham, D. M. Ferguson, G. L. Seibel, U. C. Singh, P. K. Weiner and P. A. Kollman, *AMBER 4.1*, University of California, San Francisco, 1995.
- 39 M. J. Frisch, G. W. Trucks, H. B. Schlegel, P. M. W. Gill, B. G. Johnson, M. A. Robb, J. R. Cheeseman, T. A. Keith, G. A. Petersson, J. A. Montgomery, K. Raghavachari, M. A. Al-Laham, V. G. Zahrzewski, J. V. Ortiz, J. B. Foresman, J. Cioslowski, B. B. Stefanov, A. Nanayakkara, M. Challacombe, C. Y. Peng, P. Y. Chen, W. Ayala, M. W. Wong, J. L. Andres, E. S. Repogle, R. Gomberts, R. L. Martin, D. J. Fox, J. S. Binkley, D. J. Defrees, J. Baker, J. P. Stewart, M. Head-Gordon, C. Gonzales and J. A. Pople, 1994 *Gaussian 94*, Gaussian Inc., Pittsburgh.
- 40 R. J. Hall, S. A. Hindle, N. A. Burton and I. H. Hillier, *J. Comput. Chem.*, 2000, **21**, 1433.
- 41 S. Huo, J. Wang, P. Cieplak, P. A. Kollman and I. D. Kuntz, *J. Med. Chem.*, 2002, **45**, 1412.
- 42 K. B. Ljungberg, J. Marelus, D. Musil, P. Svensson, B. Norden and J. Åqvist, *Eur. J. Pharm. Sci.*, 2001, **12**, 441.
- 43 T. Hansson and J. Åqvist, *Protein Eng.*, 1995, **11**, 1137.
- 44 J. J. P. Stewart, *J. Comput. Chem.*, 1989, **10**, 209.
- 45 A. D. Becke, *J. Chem. Phys.*, 1993, **98**, 5648.
- 46 C. Lee, W. Yang and R. G. Parr, *Phys. Rev. B*, 1988, **37**, 785.
- 47 R. V. Stanton, M. Perakyla, D. Bakowies and P. A. Kollman, *J. Am. Chem. Soc.*, 1998, **120**, 3448.
- 48 V. Daggett, S. Schroder and P. A. Kollman, *J. Am. Chem. Soc.*, 1991, **113**, 8926.
- 49 T. Ishida and S. Kato, *J. Am. Chem. Soc.*, 2003, **125**, 12035.